Automatic Generation Control of Renewable Energy Based Multi-Area System with Plug in Electric Vehicle

Subhranshu S. Pati *, Aurobindo Behera **‡, Tapas K. Panigrahi***

*Department of Electrical Engineering, Vijayanjali Institute of Technology, Balasore, Odisha, India, 756043

**Department of Electrical Engineering, Cambridge Institute of Technology, Ranchi, Jharkhand, India, 835103.

***Department of Electrical Engineering, Parala Maharaja Engineering College, Berhampur, Odisha, India, 761003.

(subhranshupati16@gmail.com, abehera2205@gmail.com, tkpanigrahi.ee@pmec.ac.in)

‡ Aurobindo Behera, Department of Electrical Engineering, CIT, Ranchi, Jharkhand, India, 835103, Tel: +91 7978422329, abehera2205@gmail.com

Received: 23.11.2019 Accepted:15.01.2020

Abstract- The work presented proposes a combination of a quick and reliable controller for the 2-area thermal system with the plug-in electric vehicle. For controlling and normalizing the system output, controlling the rotational frequency of the generator is an effective technique. A multi-constrained function is effective but the new objective function formulated is further effective and has been used in the optimization process with Intelligent Water Drops (IWD) algorithm for tuning the controllers. The performance with n filter integrated Proportional Integral Derivative (nPID) controller in the proposed system has been compared to structures such as PID and PI for validation of the effectiveness with step and dynamic load variation. Statistical analysis such as Analysis-Of-variance (ANOVA) is also performed. The work is extended by integrating wind turbines and tested with a variation of 10% in step loading and ±5% in dynamic loading of 120/80 seconds for either area. A significant improvement in response time is witnessed.

Keywords- Automatic Generation Control (AGC), Analysis of Variance (ANOVA), Intelligent Water Drops (IWD) algorithm, Plug in Electric Vehicle (PEV), Renewable Energy.

1. Introduction

The power demand by the human civilization is reaching new heights. The increase in power requirement is needed to be handled keeping in mind the future requirements. A mere increase in generated power is not the solution, rather the overall power system network has to be remodeled. This increases the complexity of the power system and brings in issues such as stability, reliability and power quality. Methods have been developed to deal with these issues effectively. One of the parameters on which the stability depends is the operating frequency of the system. The deviation on frequency is handled by the AGC by controlling the governor output to the turbine, thus controlling the rotational speed of the machine to maintain the frequency under nominal limits. For a custom functioning of an electrical power system, the frequency and voltage must be kept under check. The interconnection of the power system areas is done to increase the efficiency of the system. But the operation of the interconnected system is biased by the frequency and most effort in the past has been done to develop a pre-controller for the governor and control the droop characteristics 'R' of the machine. Many classical, heuristic and artificial intelligent techniques have been developed to calculate the optimized parameter value for the pre controller so as to minimize the frequency variation subjected to change in loading [1,2].

Techniques such as classical method centered optimization technique fulfil its objective of optimizing the controller parameters, but these techniques demonstrated are awfully time-consuming if multiple factors are augmented at the similar instant of time. In related works, the Integral Square Error (ISE) and Integral Time Absolute Error (ITAE) criterion is implemented for obtaining the primary numerical values of the resulting parameters [3, 4]. Nature-inspired Algorithms reveal their capability to resolve optimization complications for different operational problems. To maintain the system operation under control different controllers such as I, PI, PID, PID2, fractional PID have been used over period. Simple optimization technique such as

Particle swarm optimization (PSO) and Pattern Swarm (PS) algorithm applied to pitch control of wind turbine with PI controller has been proposed by Behera et. al. [5] and application of a fuzzy adaptive cascaded PID controller has been proposed by Fadaei et. al. [6]. Several hybrid techniques such as PSO-LEVY flight algorithm applied to a fuzzy-PID controller for multi-area systems have been proposed by Barisal et. al. [7] and a time-frequency method inspired fuzzy logic system for detecting Power Islands suggested by Dash et. al. [8] has provided better operating response by combining the advantages of different techniques. A comparision of modified PSO and firefly algorithm for PV system has been presented by Elrheem et.al. [9]. Also, tuning the control parameters is relatively complicated, as the combination of multiple techniques increases the response time in certain cases. The IWD algorithm developed from the flow of water particles in a stream is applied in the problem for achieving some improved result considering the ITAE criterion.

It can be perceived from past works that the deviation of several quantities, particular frequency is one of the main concerns in non-conventional power stations. And, this can be overcome by implementing the AGC scheme. The ultimate objective of AGC is to preserve the balance between total generations and net demand; otherwise the whole system may go to state of cascaded blackout [10]. The plugged-in-electric-vehicle (PEV) has great potential in near future in various ancillary services such as primary frequency control. On the other hand its popularity is increasing day by day as dependency on fossils fuel is decreasing and harmful effect of contaminated gas like carbon dioxide and ozone gases on the environment. Owing to above said benefits of PEV, authors have been motivated to include PEV in the AGC study. Furthermore, to make the thermal-hydro power plant more real-world different nonlinearities have been involved in the power plant, i.e. Constrained Rate of Generation (GRC), Dynamics of Boiler (BD) [11] and Dead Band of Governor (GDB) [12]. The inclusion of non-linearities makes the system design more complex and requires an improved control action. However, selecting a fast as well as accurate optimization technique and suitably adjusting the parameters for the controller would stabilize the system when subjected to disturbances [13]. For tuning the controller parameters, various optimization techniques are suggested by the past literatures. Some are genetic algorithm (GA), PSO, differential evolutionary (DE) algorithm. It is reported that, some of the presented algorithms have suffered from severe limitations and consumed over time than the decided limit. That's why authors used recent and effective optimization algorithm called as IWD in this study [14].

The AGC in the interconnected 2-area thermal system has 3 basic control actions.

- The control of the rotational frequency so as to keep the frequency within limits for stable operation.
- Facilitate proper interchange of power through the interconnection between the 2-area systems.
- Schedule a Cost effective generation of power by each unit.

The control action by the AGC can provide voltage control as well as frequency control for the system as the basic control action is provided by governor which regulates the steam to the turbine. The electrical frequency is proportional to the rotational frequency in a conventional power system and so is the magnitude of voltage. The variation in load affects the system frequency but the system should be capable of returning to the acceptable state of equilibrium. The model is divided into 2 basic loops, the prime loop to control valve setup in the speed governor by sensing the turbine rotation speed and the auxiliary loop performs the control action of the output frequency and power to be traded via the tie-line. The performance of the system (i.e. ΔF_1, ΔF_2, ΔP_{tie}) is studied with different loading condition for developing a robust network. The system modelling in Fig.1 considers certain non-linarites (i.e. GDB, BD) to realize the actual operating environment for precise analysis. The boiler parameters (i.e.K_1, K_2, K_3, K_{IB}, T_{IB}, T_{RB}, T_F and C_B) are considered for variation of the boiler dynamics in Fig.1. A variation of 30% of each parameter is done simultaneously to simulate a variation in boiler dynamics for testing of the robustness of the system which has been presented in section 6 of the paper.

The power demand by the human civilization is reaching new heights. The increase in power requirement is needed to be handled keeping in mind the future requirements. A mere increase in generated power is not the solution, rather the overall power system network has to be remodelled. This increases the complexity of the power system and brings in issues such as stability, reliability and power quality. Methods have been developed to deal with these issues effectively. One of the parameters on which the stability depends is the operating frequency of the system. The deviation on frequency is handled by the AGC by controlling the governor output to the turbine, thus controlling the rotational speed of the machine to maintain the frequency under nominal limits. For a custom functioning of an electrical power system, the frequency and voltage must be kept under check. The interconnection of the power system areas is done to increase the efficiency of the system. But the operation of the interconnected system is biased by the frequency and most effort in the past has been done to develop a pre-controller for the governor and control the droop characteristics 'R' of the machine. Many classical, heuristic and artificial intelligent techniques have been developed to calculate the optimized parameter value for the pre controller so as to minimize the frequency variation subjected to change in loading [1,2].

Techniques such as classical method centred optimization technique fulfil its objective of optimizing the controller parameters, but these techniques demonstrated are awfully time-consuming if multiple factors are augmented at the similar instant of time. In related works, the Integral Square Error (ISE) and Integral Time Absolute Error (ITAE) criterion is implemented for obtaining the primary numerical values of the resulting parameters [3, 4]. Nature-inspired

Algorithms reveal their capability to resolve optimization complications for different operational problems. To maintain the system operation under control different controllers such as I, PI, PID, PID2, fractional PID have been used over period. Simple optimization technique such as Particle swarm optimization (PSO) along with Fuzzy has been proposed by Khaehintung et. al. [5] and application of a fuzzy adaptive cascaded PID controller being proposed by Fadaei et. al. [6]. Several hybrid techniques such as PSO-LEVY Flight Algorithm Based Fuzzy PID Controller for Automatic Generation Control of Multi Area Power Systems proposed by Barisal et. al. [7] and a hybrid time-frequency approach based fuzzy logic system for power island detection in grid connected distributed generation proposed by Dash et. al. [8] has provided better operating response by combining the advantages of different techniques. Also, tuning the control parameters is relatively complicated, as the combination of multiple techniques increases the response time in certain cases. The IWD algorithm developed from the flow of water drops in a river is applied in the problem for achieving some improved result considering the ITAE criterion.

It is observed from past literature that, the deviation of various quantity particular frequency is one of the major concerns in renewable based power plant. This problem is overcome by adopting the concept of AGC. The fundamental mechanism of AGC is to maintain the balance between generations and demand otherwise the whole system may go to state of cascaded blackout [9, 10]. The plug in electric vehicle (PEV) has great potential in near future in various ancillary services such as primary frequency control. On the other hand its popularity is increasing day by day as dependency on fossils fuel is decreasing and harmful effect of contaminated gas like carbon dioxide and ozone gases on the environment. Owing to above said benefits of PEV, authors motivates to include PEV in the AGC study. Furthermore, to make the thermal-hydro power plant more real-world different nonlinearities involved in the power plant named as Generation Rate Constraint (GRC), Boiler Dynamics (BD) and Governor Dead Band (GDB) is reflected in the study but it makes the controller design more complex and critical. However, selecting appropriate tuned controller, the system becomes stable when subjected to disturbances [11, 12]. For tuning the controller parameters, various optimization techniques are used suggested by the past literatures. Some are Genetic Algorithm (GA) Particle Swarm Optimization (PSO), Differential Evolutionary (DE) algorithm. It is reported that, some of presented algorithm suffer from limitations and consume more time than the pre-determined limits. That's why authors used recent and effective optimization algorithm called as intelligent water drops algorithm (IWD) in this study [13, 14].

The AGC in the interconnected 2-area thermal system has 3 basic control actions.

- The control of the rotational frequency so as to keep the frequency within limits for stable operation.
- Facilitate proper interchange of power through the interconnection between the 2-area systems.
- Schedule a Cost effective generation of power by each unit.

The control action by the AGC can provide voltage control as well as frequency control for the system as the basic control action is provided by governor which regulates the steam to the turbine. The electrical frequency is proportional to the rotational frequency in a conventional power system and so is the magnitude of voltage. The variation in load affects the system frequency but the system should be capable of returning to the acceptable state of equilibrium. The model is divided into 2 basic loops, the prime loop to control valve setup in the speed governor by sensing the turbine rotation speed and the auxiliary loop performs the control action of the output frequency and power to be traded via the tie-line. The performance of the system (i.e. ΔF_1, ΔF_2, ΔP_{tie}) is studied with different loading condition for developing a robust network. The system modelling in Fig.1 considers certain non-linarites (i.e. GDB, BD) to realize the actual operating environment for precise analysis. The boiler parameters (i.e.K_1, K_2, K_3, K_{IB}, T_{IB}, T_{RB}, T_F and C_B) are considered for variation of the boiler dynamics in Fig.1. A variation of ±30% of each parameter is done simultaneously to simulate a variation in boiler dynamics for testing of the robustness of the system which has been presented in section 6 of the paper.

2. Design and configuration of the studied system

Figure.1 shows blocks with B_1 and B_2, R_1 and R_2 are parameters for biasness of frequency and governor regulation in p.u respectively.; area control error in area-1 (ACE_1) and area-2 (ACE_2), u_1 and u_2 the control errors for both areas and the controller signal for governor control; T_{g1} and T_{g2}, T_{t1} and T_{t2}, T_{P1} and T_{P2} are the time constants (sec) for Governor, Turbine, power system respectively; ΔP_{G1} and ΔP_{G2}, ΔP_{T1} and ΔP_{T2}, ΔP_{D1} and ΔP_{D2}, ΔP_{Tie} are the incremental power change in p.u. for the output command from governor, output of the turbine, load demand For each area and interconnected tie line for the 2 areas; T_{12} the exchange synchronizing coefficient and ΔF_1 and ΔF_2 the frequency deviations for individual areas (Hz) . The input to the plants are ACE and controller signal, similarly output is frequency deviation of respective control area. Relevant parameter values have been considered as in [13, 15].

2.1. Base load plants

A PEV integrated 2-area hydro-thermal system is considered in the study and nPID controllers are used to control and regulate the overall system. The generalized block diagram with transfer function is shown in Fig.1(a). To make the system more realistic, appropriate non linarites such as GRC, GDB and BD is considered in the hydro-thermal system. Generally, BD is used to produce super saturated steam that runs the turbine. When there will be variation in steam, BD respond it effectively by taking corrective action. GDB is a fixed amount of time in which governor and valves operated after certain amount of time due to presence of mechanical linkages. GDB of 0.02% and 0.05% is considered in hydro and thermal systems respectively. On similar note, the rise/fall of generation is coordinate at a fixed rate known as GRC. 3% of GRC is considered in the thermal unit. For hydro unit, rising the generation is achieved at a rate of 270% and lowering the generation at 360% per minute.

2.2. PEV system

With advancement of technology, PEV is an emerging research area with objective of making conventional grid into smart grid [15]. In this study, an aggregate model of PEV taken into consideration whose transfer function model has been described in Fig.1(b). Normally, PEV comprises of primary frequency control, load frequency controller and battery charger as displayed in Fig 1 (b). The detailed working of each system component can be referred from the literature presented in reference section [15, 20]. It is observed that, PEV not only takes part in AGC but also have great potential in ancillary services. In this paper 2000 PEV units are utilized per control area. The power rating of each PEV unit is 5KW but its range may increase up to 50KW. However, rest parameters are referred from Debbarma et al.

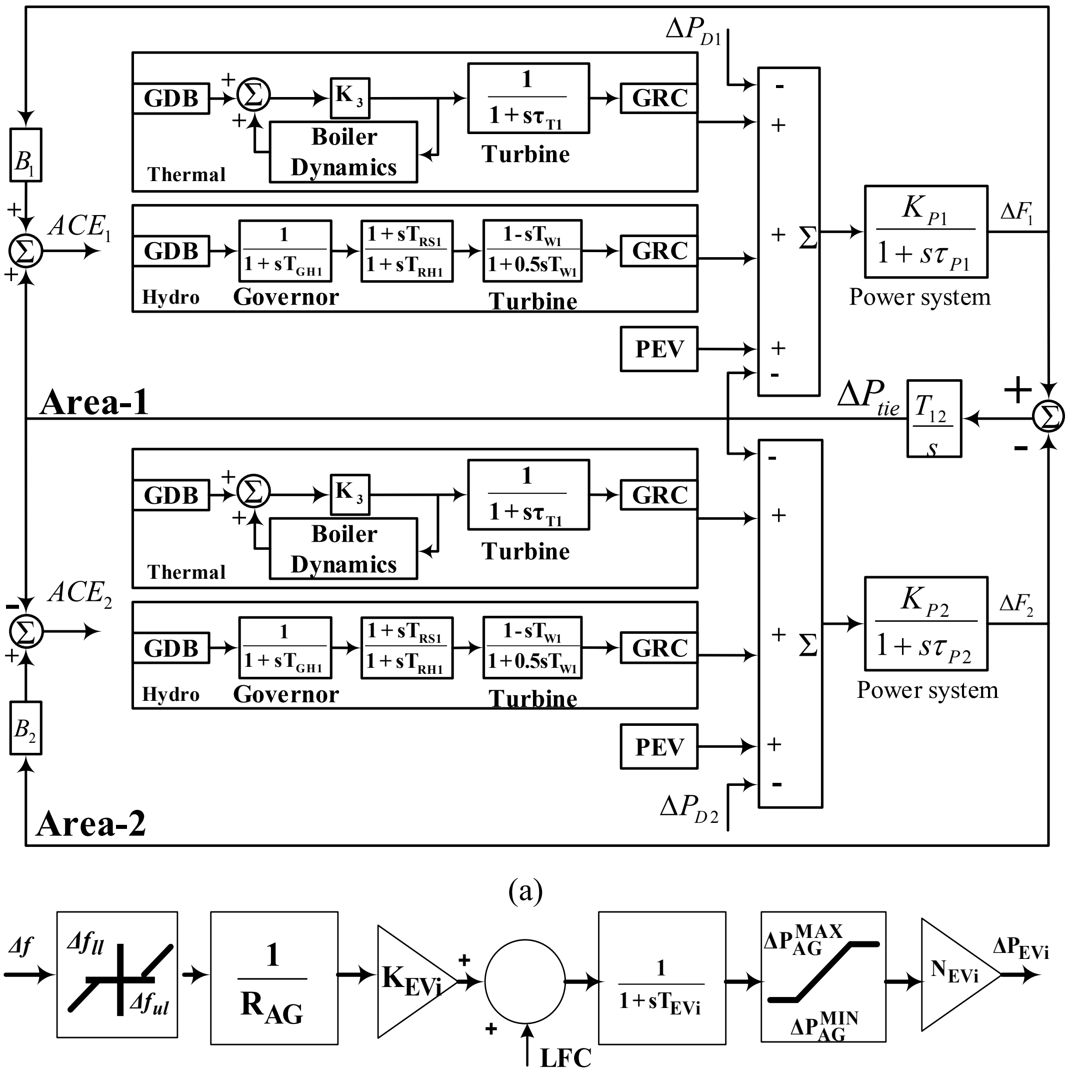

(a)

(b)

Fig. 1. (a) The 2-area hydro-thermal system transfer function model, (b) Transfer function model of PEV

3. Controller and objective function

For effectively controlling of the test system, nPID controller is used in the following paper. The basic constructional structure of nPID controller is depicted in Fig.2 in which K_p, K_i and K_d represents proportional, integral and derivative gains respectively. An additional Filter coefficient (N) is also present in the used controller. Based on the difference of present outputs with respect to desired output, a correction factor is evaluated and is considered as the input to the controller. These type controllers can be found in process in which controlling of temperature, pressure, flow and other process variables are involved.

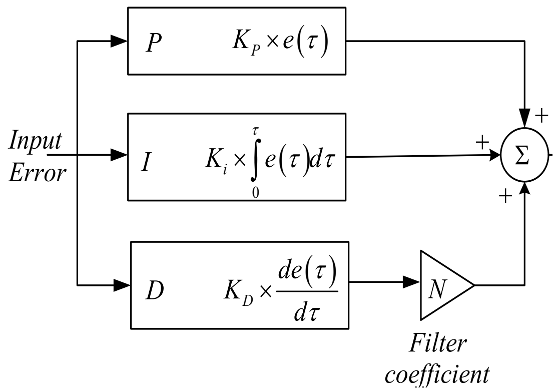

Fig. 2. Controller applied for the system considered

However, the proportional term is used for modifying the control signal proportional to the difference of actual and desired output. Thus, the desired output cannot be achieved because, as the difference reaches zero, so does the correction factor. This problem is overcome by use of integral gain in the present work. It effectively modifies the error value obtained from the proportional action to raise the correction factor. In some cases, it try to reduce the cumulative error to zero even if, the target value is achieved, resulting an overshoot in system. Derivative action minimizes this overshoot by decelerating the correction factor applied as the response come close to target value. The filter presents in the controller attempts to reduce the unwanted noise and higher order frequency caused by the controller switching action of nPID controller. So that, the inner oscillations produced from the operation decreases and the overall system stability improves to great extent. The input to the controller $U_1(s)$ and $U_2(s)$ are applied to the corresponding power plants. The transfer function for the above discussed controller is presented in Eq. (1). In Eq. (2) and (3) the Area Control Error for area-1 and area-2 respectively, has been discussed. The ACE_1 and ACE_2 act as error inputs to the controller.

$$TF_{nPID} = \left[K_P + K_i \left(\frac{1}{s} \right) + K_D \left(\frac{N_s}{s+N} \right) \right] \quad (1)$$

$$ACE_1 = \Delta P_{tie} + B_1 \Delta F_1 \quad (2)$$

$$ACE_2 = -\Delta P_{tie} + B_2 \Delta F_2 \quad (3)$$

The input to the controller of both areas is ACE_1 and ACE_2 respectively [10, 13]. The ITAE has to model so as to use in the optimization procedure. Over the past years of these four criterions (i.e. Integral Time Square Error (ITSE), ISE, Integral Absolute Error (IAE), ITAE), ITAE is the most prominently used criterion.

$$J_1 = POS_{\Delta f_1} + POS_{\Delta f_2} + POS_{\Delta P_{Tie}} \quad (4)$$

$$J_2 = T_{S\,\Delta f_1} + T_{S\,\Delta f_2} + T_{S\,\Delta P_{Tie}} \quad (5)$$

$$J_3 = ITAE = \int_0^{t_{sim}} (|\Delta F_1| + |\Delta F_2| + |\Delta P_{tie}|).t.dt \quad (6)$$

$$J(J_1, J_2, J_3) = \omega_1 J_1 + \omega_2 J_2 + \omega_3 J_3 \quad (7)$$

The Eq. (4) - (6) are individual objective functions which are combined to form a single objective function in Eq. (7). The individual Eq. (4) - (6) represent the summation of the peak overshoot (POS), Settling time (T_S) of frequency deviation for each area as well as the deviation in power exchange and the ITAE error function respectively. The weights of the individual function values (J_1, J_2, and J_3) are presented by ω_1, ω_2 and ω_3 which determine their contribution to the final objective function value (J). The value 0.75, 0.18 and 0.07 is chosen for ω_1, ω_2 and ω_3 respectively. It is done by the implementation of Analytic Hierarchy Process (AHP) as suggested by Singh et. al. in [16].

4. Description of the optimization technique: IWD

Intelligent water drops (IWD) optimization, a smarm centered technique proposed by shahhosseseni [14]. The algorithm is inspired by flow of water drops in the stream. The algorithm step imitates the reaction mechanism of molecules of water as they flow in the river. While execution of the algorithm, water drops work together to produce enhanced solution either for minimization or maximization problem. Hence, this is a population oriented algorithm for generation of optimal solution. It also shows improved results when applied to different research area like travelling salesmen and multidimensional knapsack problems. It has two major characteristics.

- The measure of soil contained currently, $soil_{IWD}$.
- The velocity for the soil particles, $velocity_{IWD}$.

In the IWD algorithm, the static and dynamic set of operators discussed has a significant effect while making the selection. Initial value of $velocity_{IWD}$ and starting soil trail has been referred as static parameters and will be fixed throughout. The dynamic parameters like visited node need to be updated in each iteration so as to obtained global optimal solution. The choice of nodes i - j are dependent on the function of edge probability and its two related functional quantity. Post completions of iteration, the dynamic parameters are reinitiated and again the processes continue till stopping criteria is reached. Generally, stopping criteria is predefined number of iterations (Max_{itr}) or until the tolerance limit for the final solution is reached. For implementing the optimization problem through IWD technique, following procedure should be followed. The maximum number of the iteration is specified by the user and the counter (Itr) is set to 0. The number of water drops (NWD) is fixed to a positive integer value which is usually decided by the number of nodes present in the graph. The global soil updating parameter is taken in the range of 0 to 1, normally taken just less than 1. Moreover, the soil on each path (edge) represent by intsoil is set such that the soil of the path between i to j is se(i;j) = int_{soil}. The velocity (int_{vel}) is also set. However, intsoil and intvel is specified by the user and adjusted through experimentally. Initialize all dynamic parameter. The IWDs are distributed evenly on all visited nodes V_c. It should be noted that all the visited nodes zero amount of soil and velocity of IWD is intvel. The visited node list is updated when all the process of one visited node is completed and following procedure is performed for further advancement.

Based on edge probability the next node is targeted and has been shown in Eq. (8) – (10).

$$\Pr o_i^{IWD} = \frac{f(soil_{i,j})}{\sum_{k \notin v_c} f(soil_{i,j})} \tag{8}$$

Such that

$$f(soil_{i,j}) = \frac{1}{\in_s + g(soil_{i,j})} \tag{9}$$

$$\begin{aligned} & g(soil_{i,j}) = soil_{i,j}; \\ & if\,(\min_{l \notin v_c}(soil_{i,j}) \geq 0) \\ & else \\ & soil_{i,j} - \min_{l \notin v_c}(soil_{i,j}) \end{aligned} \tag{10}$$

Algorithm 1: IWD Algorithm
1. Step 1 Initialization process
2. a. Initialise the counter (Itr) to 0.
3. b. Initialise the edge soil & velocity of IWDs.
4. c. Initialise all the static and dynamic parameters.
5. Step 2:
6. While (itr < Max_{itr})
7. Formulate new solutions by using Eq. (8) to (15).
8. If (rand > pulse rate) then
9. Identify best solution from poll of solutions. Formulate a local search using best solution.
10. Generate new solution arbitrarily
11. If (rand < l_i & f(obj) < f(e_i)) then
12. New solution and increase pulse rate while decreasing loudness
13. Rank them and identify the current best e_i.
14. Select the best $X_{j,\,best,\,i}$ and worst $X_{j,\,best,\,i}$ from the whole solution.
15. Generation of new population: By following equation 3, current solution $X_{j,\,k,\,i}$ is revised to generate new sol. $X''_{j,\,k,\,i}$ subjected to best and worst solution.
16. Fitness valuation of new solution :
17. If J(X_0) ≤ J(X) then
18. Revised the previous parameter with new one $X''_{j,\,k,\,i}$.
19. Else
20. No change of parameter is permitted.
21. Termination criteria verified: If no of iteration is less than the pre-defined limit.
22. Then: Goto → Step 2.

The new Velocity vel(t + 1) is updated with using old velocity vel(t) by following Eq. (11). Where a_v, b_v and c_v are velocity updating parameters and taken as 1, .01 and 1 respectively.

$$vel(t+1) = vel(t) + \frac{a_v}{b_v + c_v soil^2_{i,j}} \tag{11}$$

The soil edge(Se) is replaced by new soil edge by referring the Eq. (12).

$$Se = Se + \Delta soil_{i,j} \tag{12}$$

The iteration-best solution T_{ib} can be found from all the solutions T_{IWD} by adhering Eq. (13).

$$T_{ib} = \arg \max_{\forall T_{IWD}} q(T_{IWD}) \tag{13}$$

Where q(T_{IWD}) is used to calculate the quality of the solution. By following the above procedure S_e, S_{PO} and Global soil propagation is updated as depicted in Eq. (14).

$$soil_{i,j} = (1+\rho_{IWD})soil_{i,j} - \rho_{IWD}\frac{1}{(N_{IB}-1)}soil^{IWD}_{i,j} \tag{14}$$

The global soil updating parameter (IWD) is a constant and lies between 0 to 1. N_{IB} represents the no of nodes in the iteration T_{ib}.

The total best solution (T_{tb}) is evaluated with using iteration best (T_{ib}) solution as shown in equation (15) and same S_e, S_{PO} and Global soil propagation is updated again if needed.

$$T_{tb} = T_{ib};\ if\ (q\ (T_{tb}) \geq q\ (T_{ib})),\ else\ T_{tb} \tag{15}$$

The iteration counter is incremented by 1 (i.e itr=itr+1) and again same procedure is repeated from step 2, if itr < Max_{itr}.

5. Result analysis and observation

In the previous literature it can observed that nPID has the ability to optimize both transient and steady state response of the performance. 0 < K_p, K_i, K_d < 2; 0 < N < 500 are the upper and lower limits of controller parameters. The test system is verified by application of 1% SLP of in area 1 and area-2. The Table 1. contains the optimal control parameter value of different controllers used, whereas, Table 2. shows the numerical comparison of performance with different controllers. The initial delay in the response is due to the governor dead band.

Table 1. Parameter values for optimized functioning of the controller by IWD.

Controller	OPTIMUM CONTROLLER PARAMETER			
	K_p	K_i	K_d	N
PI	0.2479	0.2160	-	-

PID	0.2826	0.4493	0.3922	-
nPID	0.1431	0.1701	0.8781	429

Table 2. System parameter values for various controllers applied to the system with 5% variation of step load.

Type of controller	Parameters of area	Overshoot/ Undershoot ($\times 10^{-3}$)	Settling time (Sec)	Steady state error ($\times 10^{-4}$)
PI	ΔF_1	-43.20	12.06	1.339
	ΔF_2	-42.80	12.13	1.271
	ΔP_{tie}	21.83	12.24	0.219
PID	ΔF_1	-41.40	11.870	-7.139
	ΔF_2	-14.50	17.103	-5.107
	ΔP_{tie}	-29.12	13.910	0.205
nPID	ΔF_1	-22.10	11.02	-0.043
	ΔF_2	-41.70	11.93	-0.129
	ΔP_{tie}	-3.720	8.968	0.062

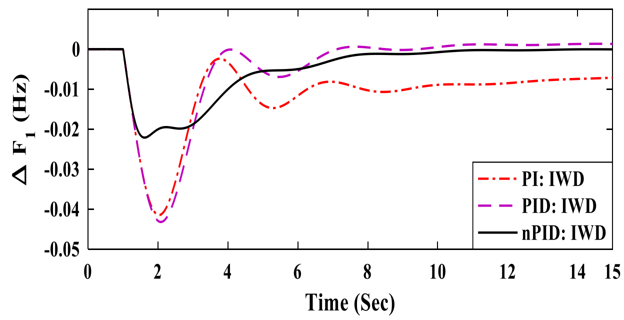

(a)

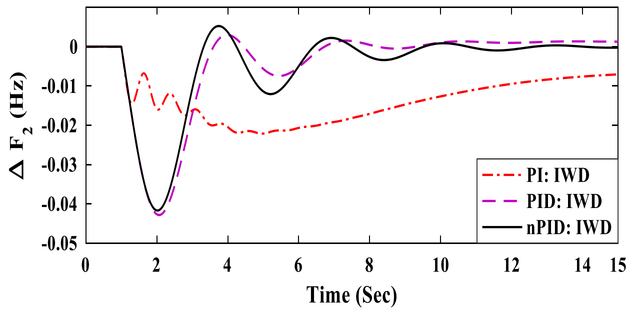

(b)

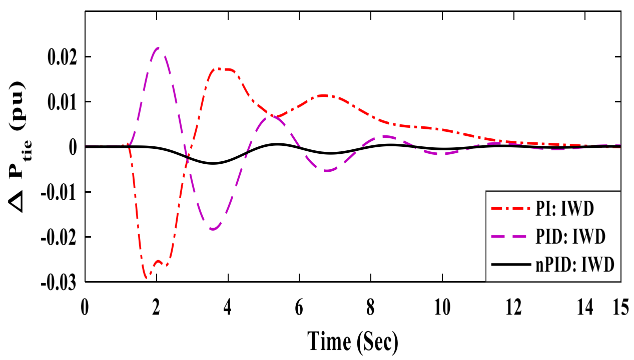

(c)

Fig. 3. System response for various types of controllers.

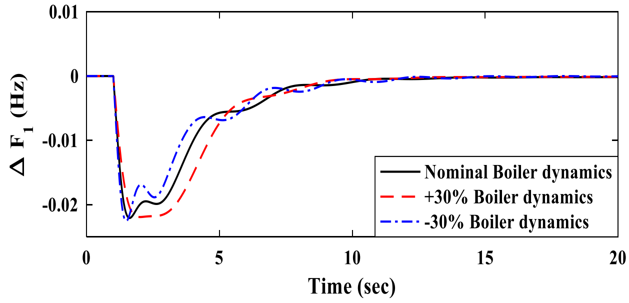

(a)

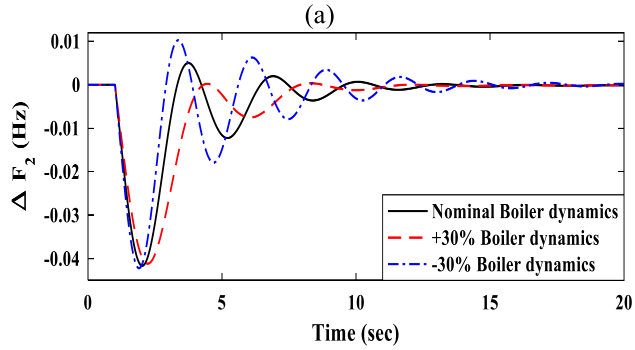

(b)

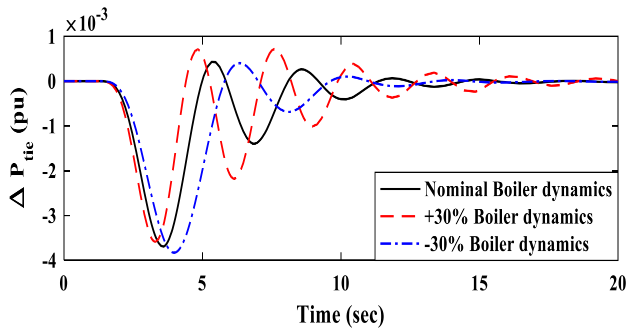

(c)

Fig. 4. Analyzing the effect of change in boiler setting.

The compatibility of various controller set has been studied of which the nPID controller produce a much better optimized performance result as can be observed from Fig.3. In Fig.3 clear improvement is observed from the curve from PID controller but a further reduction in overshoot, settling time and steady state error is observed by application of nPID controller to the studied system.

Table 3. holds a breakdown of the data set, into its major system/performance parameters (i.e. Over Shoot (OS), Settling Time (T_s), and Sready State Error (E_{SS})) , used for the purpose of statistical analysis. Best, mean, worst and standard deviation (SD) for each system parameter has been discussed. For making a statistical analysis various performance parameters were recorded for each controller and their respective frequency deviation for area-1 and area-2 as well as the tie line exchange power. It can be observed from the table that the best solutions are obtained for the same set of controller settings. Rather based on the objective function value as per equation (5-8) the solution with best objective function value is chosen as the obtained optimized solution. But due to its ability to

limit the transient response, nPID controller provides an optimum solution to the stability issue.

The statistical analysis of the individual as well as the combined objective function value shows the effectiveness of the proposed controller for the system considered. Further ANOVA is applied to the obtained result for 50 test runs, which further ensures the validity and effectiveness of the scheme for maintaining a stable operation even during load variation. For implementation of ANOVA to the problem the model was tested 10 times with each controller being tuned by IWD technique. The response is evaluated on the basis of the objective function value obtained being presented in Table 4. Table 4. holds the data set for implementing ANOVA and Table 5. displays the result obtained. In Table 5 it can be observed that the F > $F_{critical}$ (i.e. F=9.8584 and Fcritical = 9.0194) and also P < 0.001 (i.e. P = 0.0006), thus the null hypotheses is rejected (i.e. $\mu_1 \neq \mu_2 \neq \mu_3$). Thus, with a confidence level of 99.99% it can be considered that the 3 different controller produce distinct result which are significantly different of which the result obtained by the proposed technique is significantly improved.

Table 3. Relative statistical breakdown for various controllers and system parameters.

	System parameters	Statistically measures	PI	PID	nPID
ΔF_1	OS	Best	0.0411	0.0408	**0.0221**
		Mean	0.0423	0.0418	**0.0296**
		Worst	0.0432	0.0426	**0.0422**
		SD×10^{-4}	6.8150	6.4045	6.4000
	Ess (×10^{-4})	Best	0.4700	7.9300	**0.0437**
		Mean	**10.205**	38.510	16.976
		Worst	**20.550**	80.010	49.500
		SD	7.0424	23.804	17.284
	T_s	Best	10.96	13.810	**7.1410**
		Mean	13.72	15.332	**8.5611**
		Worst	17.22	17.800	**11.590**
		SD	2.3595	2.6565	1.3370
ΔF_2	OS	Best	0.0413	0.0145	**0.0410**
		Mean	0.0422	0.0235	**0.0421**
		Worst	0.0433	0.0405	**0.0431**
		SD×10^{-4}	7.38	119.00	**6.87**
	Ess (×10^{-4})	Best	2.7500	8.1610	**0.1060**
		Mean	19.061	39.842	**17.149**
		Worst	**40.560**	78.770	49.520
		SD	**14.532**	23.534	17.086
	T_s	Best	11.720	**9.1800**	9.6580
		Mean	13.383	12.949	**12.086**
		Worst	**15.210**	15.830	15.860
		SD	**1.3137**	2.5866	2.1338
ΔP_{tie}	OS	Best	6.08 ×10^{-4}	33.00 ×10^{-4}	**2.34 ×10^{-4}**
		Mean	0.0147	0.0199	**0.0060**
		Worst	0.0224	0.0292	**0.0166**
		SD×10^{-4}	80.00	112.00	**52.00**
	Ess (×10^{-4})	Best	**0.0675**	0.2337	0.0706
		Mean	**0.1400**	1.5147	2.6713
		Worst	**0.4813**	3.7960	4.9900
		SD	**0.1685**	1.1346	2.1853
	T_s	Best	9.3100	12.120	**9.0200**
		Mean	11.010	13.619	**10.443**
		Worst	**12.410**	15.060	15.520
		SD	**1.0507**	1.1074	1.9676
	J_1	Best	34.020	39.630	**30.040**
		Mean	38.120	41.862	**36.086**
		Worst	42.380	44.930	**38.970**
		SD	3.2134	**2.3368**	3.0707
	J_2	Best	12.236	16.324	**0.2671**
		Mean	29.406	79.866	**27.797**
		Worst	72.081	160.01	**59.561**
		SD	28.927	47.582	**28.024**
	J_3	Best	0.0866	0.0800	**0.0650**
		Mean	0.0991	0.0851	**0.0778**
		Worst	0.1082	**0.0879**	0.0902
		SD	0.0081	0.0021	**0.0012**
	J	Best	30.419	32.704	**22.582**
		Mean	33.890	45.778	**33.874**
		Worst	39.179	60.548	**42.460**
		SD	**3.0439**	9.6024	6.4875

Table 4. Data set for distinct runs and output result for ANOVA test for testing the significance of various controllers.

Controller type	Objective function Value (J) for 10 best runs									
PI	30.4	39.1	33.5	33.5	35.4	34.6	36.5	30.9	31.1	30.6
PID	32.7	60.5	51.3	50.9	47.1	46.1	46.4	34.7	33.7	55.1
nPID	22.5	31.6	40.4	42.4	37.8	31.7	29.8	29.2	31.0	41.8

Table 5.ANOVA table with p=0.1%.

Source	SS	df	MS	*F*	$F_{critical}$	*p*-value
Between	943.51	2	471.76	9.858	9.019	0.0006
Within	1292.04	27	47.853			
Total	2235.55	29				

Table 6. Robustness analysis for the system with ±30% variation in boiler parameters.

Parameter	% Variation	Undershoot (×10^{-2})	Settling time (Sec)	Steady state error (×10^{-3})
	0	-22.10	11.02	-0.026
ΔF_1	-30	-22.49	11.53	-0.036
	+30	-21.92	10.52	-0.018
ΔF_2	0	-41.70	11.93	-0.129
	-30	-42.20	12.79	0.194

	+30	-41.15	11.30	-0.118
	0	-36.92	13.70	0.062
ΔP_{tie}	-30	-38.29	12.33	-0.0117
	+30	-35.81	16.45	0.0046

Further, robustness analysis is done to determine the effect of change in boiler dynamics on the response of the system with same controller settings. A variation of ±30% is done in the boiler parameters and it can be concluded from the graphical Fig.4 and Table 6. of frequency deviation of both areas as well as the tie-line exchange power that used controller is capable of sustaining wide range variation in the system.

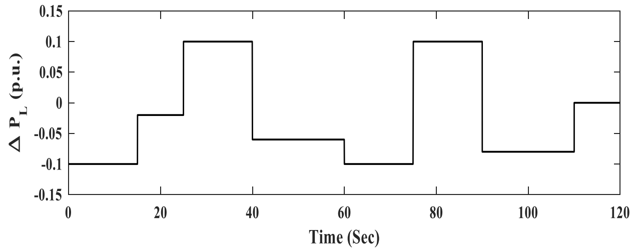

Fig. 5. The considered dynamic input for system testing.

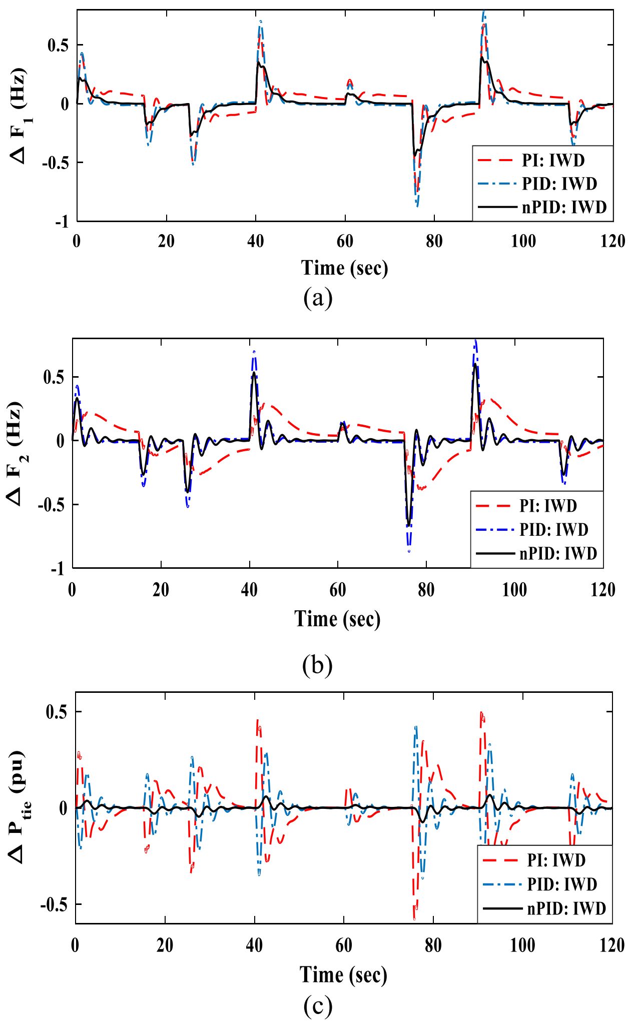

Fig. 6. System response for Dynamic load variation.

Table 7. Performance parameters for different controller in the system with Dynamic load variation up to maximum of 20%.

Type of controller	Parameters of different area	Under shoot ($\times10^{-2}$)	Settling time (Sec)	Steady state error ($\times10^{-3}$)
PI	ΔF_1	-87.77	10.96	1.35
	ΔF_2	-87.02	12.31	12.70
	ΔP_{tie}	-36.59	10.75	0.4194
PID	ΔF_1	-76.74	14.88	-77.17
	ΔF_2	-38.23	-	-75.45
	ΔP_{tie}	-58.19	13.09	-2.167
nPID	ΔF_1	**-44.23**	**9.64**	**-1.23**
	ΔF_2	**-66.62**	**11.38**	**-0.0869**
	ΔP_{tie}	**-7.43**	**9.02**	**-0.0696**

For further testing the ability of the controller to operate in a practical operating condition a dynamically varying load change of 20% in Fig.5 is applied to the system and the superiority can be observed with respect to the other controllers. Superiority of suggested controller can be concluded from Table 7. and Fig.6 which shows the response of the system to the dynamic load variation.

5. Extension of the work by integrating wind turbine

Due to burning of fossil fuel in the conventional thermal plant, greenhouse gas generated which pollute the environment. Hence it urgent need to incorporate renewable base plant like solar [17], wind [18, 19], etc. in the system which also reduced the dependency on the fossil fuel consumption plant. Impact of integrating renewable energy to the existing system is analyzed by implementation of wind turbine system to the system described in Fig.3. In Fig.7 the configuration of the system post integration is presented. Here, the thermal and hydro units have the non-linearities discussed in Section-2. The various mathematical aspects of the wind turbine is discussed in the following section.

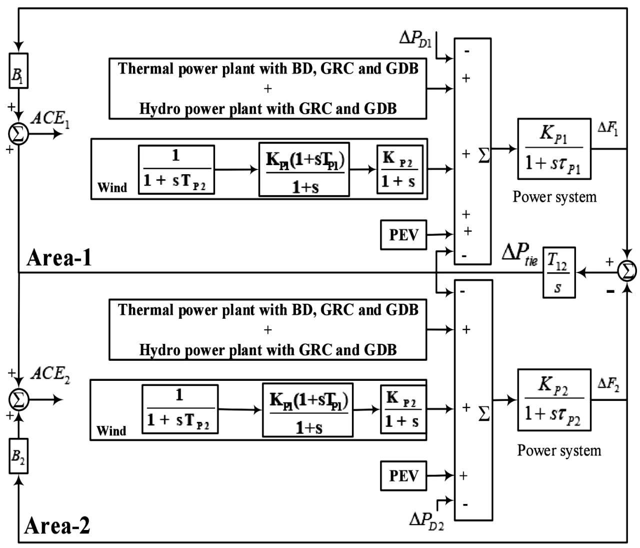

Fig. 7. Modified system configuration by integration of wind turbine to the existing system.

6.1 Wind system

Due to concern on global warming and its effect on the atmosphere, wind power plant becomes one of natural choice in wind availability region. Its popularity is increasing in renewable energy sector because it generates clean and green power. Although, wind power plant has certain limitations but they can be easily overcome with advancement in technology. A generalized transfer function hydraulic pitch actuated linear wind turbine generator is depicted in Eq. (16). As T_k is small with compared to T_{P1}, hence T_k is neglected and Eq. (16) becomes,

$$\frac{\Delta H(s)}{X(s)} = \frac{K_{P1}(1+sT_{P1})}{(T_k s^2 + sT_{P1} + 1)(1+s)} \qquad (16)$$

$$\frac{\Delta H(s)}{X(s)} = \frac{K_{P1}(1+sT_{P1})}{(1+sT_{P1})(1+s)} \qquad (17)$$

The data fit pitch response is expressed as:

$$\frac{\Delta H(s)}{X_1(s)} = \frac{K_{P2}}{1+s} \qquad (18)$$

6. Result and analysis with integration of wind plant

The test system under the analysis has diverse sources such as thermal-hydro system, wind power plant accompanied by PEV's. IWD optimized nPID controller has been employed controlling the overall system. The system is analyzed under two distinct cases;

Case-III: SLP of 10% for either area at t= 0 sec.

Case-IV: A variation (-5%; +3%; +7% and -8%) of load with respect to time (t = 0; 30; 50 and 60 seconds), has been considered and graphically presented in Fig.8.

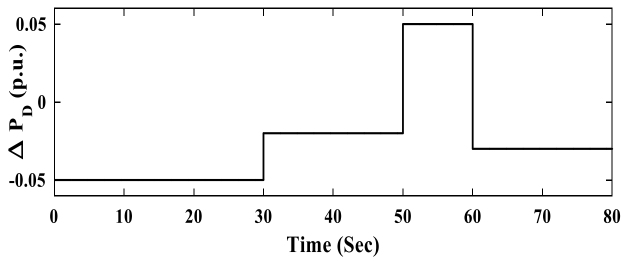

Fig. 8. Application of time varying load disturbances on the test system.

In Fig.9 the magnitude and phase angle plot for the wind integrated system has been presented and Table 8. presents the Eigen values analysis. The various IWD optimized controller parameters have been presented in Table 1. Graphical response showing the comparable analysis of PI, PID and nPID controller is shown in Fig.10. And in Fig.11 for time varying load deviation. A relative performance assessment of the used nPID controller to that of other controller for Case-III has been performed in Fig.10 and Table 9. In Fig.11 graphical response for application of time varying load disturbance as discussed in Case-IV has been presented. Table 10. is the mathematical analysis of Fig.11.

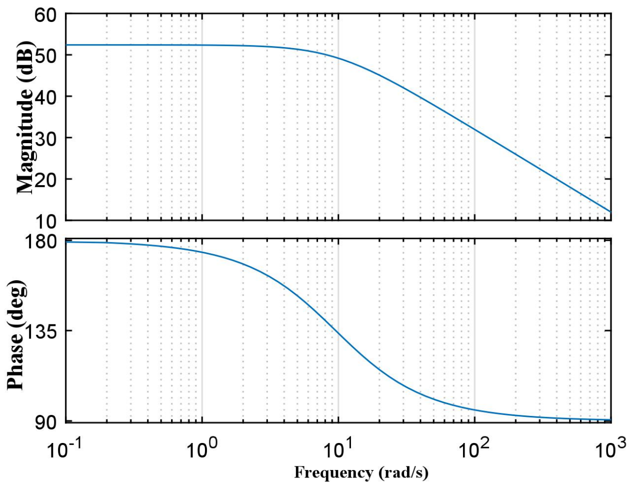

Fig. 9. Magnitude and Phase plot of the test system

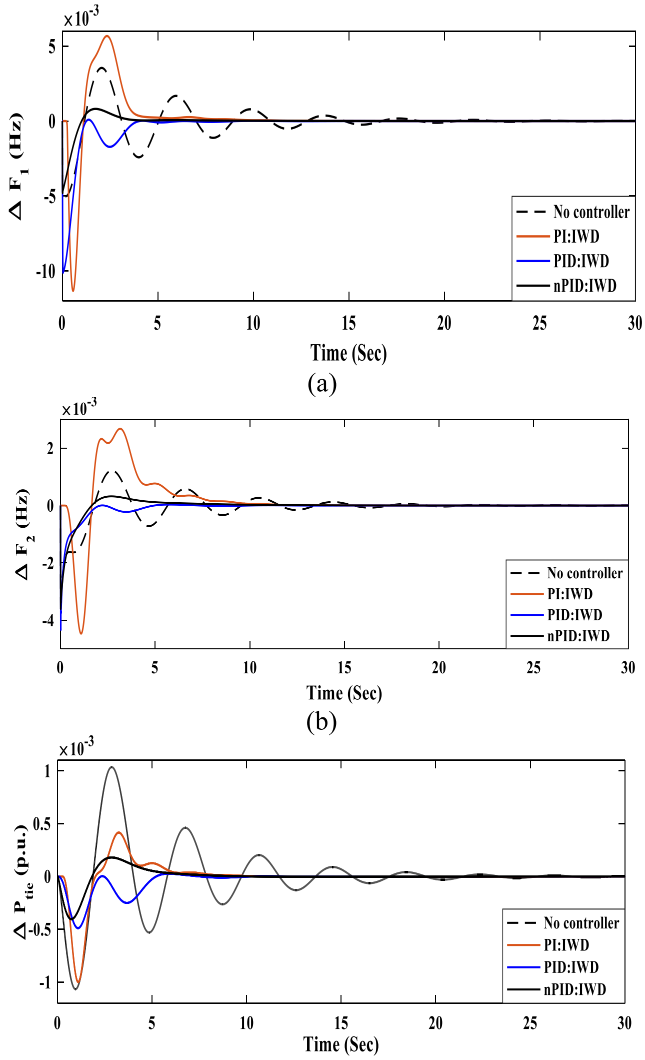

(c)

Fig. 10. Step response for variation of 10% in either area.

Table 8. Eigen Value Analysis

Eigen Value	Min. Value of damping ratio (ξ)	Min. Value of freq. of oscillation (ω_n)
-4.3905, -0.0200, -0.0010, -0.0002, -0.0200, -0.0010, -4.3905, -0.033, -4.3905, -2.1927 ± 0.7481i, -2.1748 ± 0.7794i, -2.1905 ± 0.4567i, -2.1762 ± 0.4795i, -2.1989 ± 0.7644i, -2.1702±0.0948i, -2.1923 ± 0.8429i, -2.1751 ± 0.8776i, -0.085 ± 0.0143i, -0.108 ± 0.0130i, -0.0239 ± 0.0114i, -0.090 ± 0.0141i, -0.027 ± 0.009i, -0.028 ± 0.008i, -0.024 ± 0.0011i, -0.012 ± 0.009i, -0.1250 ± 0.007i	0.9026	0.0141

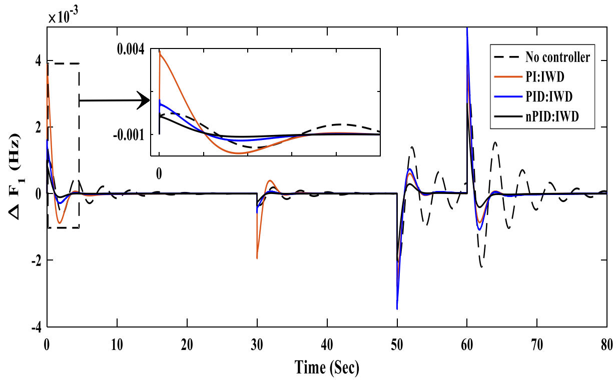

(a)

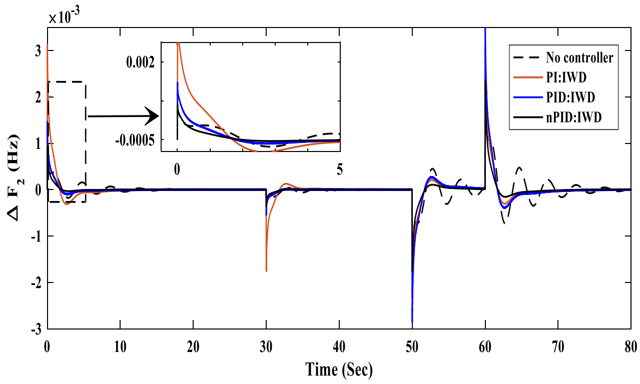

(b)

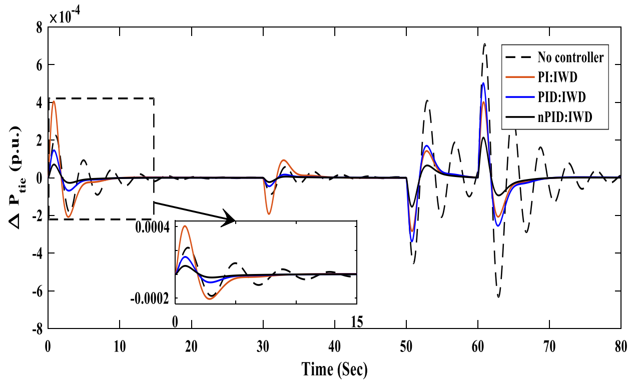

(c)

Fig. 11. Dynamic system response for case-IV.

Fig. 12. Mathematical indices of ΔF_1, ΔF_2 and ΔP_{tie} for Case-III

Techniques	Settling time (2%) T_s(S)			Undershoot (US) ($\times 10^{-3}$)		
	ΔF_1	ΔF_2	ΔP_{tie}	ΔF_1	ΔF_2	ΔP_{tie}
No controller	21.07	20.66	24.96	5.018	3.830	1.068
PI:IWD	8.499	10.52	9.775	11.33	4.471	0.995
PID:IWD	6.454	8.135	8.349	10.12	4.342	0.489
PI-PD [20]	12.37	12.24	17.81	21.45	12.16	3.550
nPID:IWD	**5.092**	**6.141**	**7.532**	**4.805**	**3.609**	**0.401**

Table 3. Mathematical indices of ΔF_1, ΔF_2 and ΔP_{tie} for Case-IV

Various operating conditions	Techniques	OVERSHOOT/ UNDERSHOOT (OS/US) ($\times 10^{-4}$)			SETTLING TIME (2%) T_s(S)		
		ΔF_1	ΔF_2	ΔP_{tie}	ΔF_1	ΔF_2	ΔP_{tie}
ΔP_D = 5% at t= 0 sec	No controller	10.23	9.64	2.23	18.35	14.52	22.7
	PI	38.73	31.21	4.05	8.828	8.969	9.82
	PID	16.12	14.70	1.45	3.593	4.595	8.82
	nPID	9.827	9.253	0.70	3.204	2.433	7.08
ΔP_D = +3% at t= 30 sec	No controller	-4.06	-3.97	-0.85	18.66	13.29	19.2
	PI	-19.4	-17.5	-1.92	7.128	7.971	10.2
	PID	-5.76	-5.51	-0.44	2.914	4.385	7.18
	nPID	-3.63	3.56	-0.22	1.826	3.262	4.69
ΔP_D = +7% at t= 50 sec	No controller	-20.7	-18.0	-4.53	NA	NA	NA
	PI	-27.8	-23.5	-2.83	4.399	6.132	6.89
	PID	-34.6	-28.5	-3.37	4.482	8.036	7.89
	nPID	-19.9	-17.6	-1.53	4.027	5.731	6.43
ΔP_D = -8% at	No controller	31.88	24.21	7.09	19.61	18.46	19.6

t= 60 sec	PI	38.53	31.02	4.01	5.327	7.021	8.69
	PID	49.63	36.35	5.02	6.691	8.823	9.54
	nPID	27.09	22.98	2.31	4.519	5.735	8.37

7. Conclusion

The work describes a comprehensive examination of the renewable source based system with PEV's, implemented with IWD algorithm optimized controller. The efficacy of the method can be realized by the fact that the degree of stability for the system has improved, even with a time varying and larger step load disturbances. The dynamic interaction of PEV with integration of distributed generations should be investigated in future. The major finding from the analysis of the test model, which is extremely complex in nature, can be highlighted as:

- Initial test with conventional system connected to PEV settles the claim of the nPID controller as the best among other controllers.
- The effectiveness of the offered nPID controller is higher to a step loading as well as continuous load variations, even with renewable integrated system.
- The IWD offers optimal tuning of the controller considering its associated parameters, thus restraining from undesirable delay in time.
- ANOVA test has been performed to statistically verify the performance of the controller and the system is operating in a stable operating condition even for 20% dynamic load variation.

References

[1]. J. Wood, B. F. Woolenberg, Power Generation Operation and Control. 3rd ed., John Wiley and Sons, 2013.

[2]. I. Elgerd, Electric energy systems theory an introduction, *McGraw-Hill Book Company*, New York, NY, 2000.

[3]. OI Elgerd, C. Fosha, "Optimum megawatt frequency control of multi-area electric energy systems", *Power Appl Syst (PAS-89)*, vol. 4, pp. 556-563, 1970.

[4]. G. Panda, S. Panda and C. Ardil, "Automatic Generation Control of Multi-Area Electric Energy Systems Using Modified GA", *World Academy of Science, Engineering & Technology*, vol. 7, pp. 576 – 584, 2013.

[5]. S. Behera, B. Subudhi, and B. B. Pati, "Design of PI controller in pitch control of wind turbine: A comparison of PSO and PS algorithm." *International Journal of Renewable Energy Research (IJRER)*, Vol. 6, No. 1, pp. 271-281, 2016.

[6]. A. Fadaei, K. Salahshoor, "A Novel Real-time Fuzzy Adaptive Auto-Tuning Scheme for Cascade PID Controllers", *International Journal of Control, Automation, and Systems*, vol. 9, pp.823-833, 2011.

[7]. A. K. Barisal, T. K. Panigrahi, S. Mishra, "A Hybrid PSO-LEVY Flight Algorithm Based Fuzzy PID Controller for Automatic Generation Control of Multi Area Power Systems: Fuzzy Based Hybrid PSO for Automatic Generation Control", *International Journal of Energy Optimization & Engineering,* vol. 6, pp. 42-63,2017.

[8]. P. K. Dash, M. Padhee, T.K. Panigrahi, "A hybrid time-frequency approach based fuzzy logic system for power island detection in grid connected distributed generation. International", *Journal of Electrical Power & Energy Systems*; vol. 42, pp. 453-464, 2012.

[9]. M. Elrheem, N. K. Bahgaat, "A Comparison Between Using A Firefly Algorithm and A Modified PSO Technique for Stability Analysis of a PV System Connected to Grid", *International Journal of Smart Grid*; vol.1, no. 1, pp. 1-8, 2017.

[10]. H. Bevrani, Robust power system frequency control, vol. 85. New York: Springer, 2009.

[11]. U. Moon, and K. Y. Lee, "Step-Response Model Development for Dynamic Matrix Control of Drum-Type Boiler-Turbine System", *IEEE Transactions on Energy Conversion*, vol. 24, pp. 423-430. 2009.

[12]. R. K. Sahu, S. Panda, G. T. Chandra Sekhar, "A novel hybrid PSO-PS optimized fuzzy PI controller for AGC in multi area interconnected power systems", *Electrical Power and Energy Systems*, vol.64, pp. 880-893, 2015.

[13]. A. Behera, T. K. Panigrahi, A. K. Sahoo, and P. K. Ray, Hybrid ITLBO-DE Optimized Fuzzy PI Controller for Multi-area Automatic Generation Control with Generation Rate Constraint. In Smart Computing and Informatics 2017, Springer, pp. 713-722, Singapore, 2018.

[14]. H. Shah-Hosseini, "Intelligent water drops algorithm: a new optimization method for solving the multiple knapsack problem", *Int. Journal of Intelligent Computing and Cybernetics*, vol.1 (2), pp.193-212 (2008).

[15]. S. Izadkhast, P. Garcia-Gonzalez, and P. FrÃas, Bauer P, "Design of Plug-In Electric Vehicles Frequency-Droop Controller for Primary Frequency Control and Performance Assessment*", IEEE Trans Power Syst,* vol. 32(6), pp. 4241-4254, 2017.

[16]. S. P. Singh, T. Prakash, V. P. Singh, M. G. Babu, "Analytic hierarchy process based automatic generation control of multi-area interconnected power system using Jaya algorithm", *International Journal of Engineering Applications of Artificial Intelligence*, vol. 60, pp. 35-44, 2017.

[17]. I. Daniel, F. Córdova, M. Avila, "Modeling and Simulation of a Solar System in the Quingeo Church in Ecuador", *6th International Conference on Smart Grid*, Nagasaki, pp. 158-163, 4-6 Dec 2018.

[18]. M. Peyman, G. N. Baltas, M. Eliassi, P. Rodríguez, "A model for flexibility analysis of RESS with electric energy storage and reserve", 7th International Conference on Renewable Energy Research and Applications, Paris, pp. 1004-1009, 14-17 Oct 2018.

[19]. P. M. Anderson, and A. Bose, "Stability simulation of wind turbine systems", *IEEE Trans Power Apparatus Syst*, vol. 102(12), pp. 3791-3795, 1983.

[20]. S. Padhy, and S. Panda, "A hybrid stochastic fractal search and pattern search technique based cascade PI-PD controller for automatic generation control of multi-source power systems in presence of plug in electric vehicles", *CAAI Transactions on Intelligence Technology*, vol.2, no.1, pp. 12-25, 2017.